El-Naggar Mehrez (Orcid ID: 0000-0003-2556-3048)

Facile production of smart superhydrophobic nanocomposite for wood coating toward long-lasting glow-in-the-dark photoluminescence

Mehrez E. El-Naggar[a*], Ali Aldalbahi[b], Tawfik A Khattab[a], Mokarram Hossain[c]

[a]Textile Research Division, National Research Center (Affiliation ID: 60014618), Dokki, Cairo, Egypt

[b]Department of Chemistry, College of Science, King Saud University, Riyadh, Saudi Arabia

[c]Zienkiewicz Centre for Computational Engineering, College of Engineering, Swansea University, SA1 8EN, United Kingdom

Abstract

Smart photoluminescent nanocomposite surface coating was prepared for simple industrial production of long-persistent phosphorescence and superhydrophobic wood. The photoluminescent nanocomposite coatings were capable to continue emitting light in the dark for prolonged time periods that may reach 1.5 hrs. Difference ratios of lanthanide-doped aluminum strontium oxide (LASO) nanoparticles immobilized into polystyrene (PS) was developed as a nanocomposite coating for wood substrates. To accomplish transparency to the prepared nanocomposite coating, LASO was efficiently dispersed in the form of nano-scaled particles to ensure homogeneous dispersion without agglomeration in the polystyrene matrix. The coated woods showed an absorption band at 374 nm and two emissive bands at 434 and 518. The luminescence spectra showed both long-persistent phosphorescence as well as photochromic fluorescence relying on the LASO ratio. The improved superhydrophobicity and resistance to scratching of the coated woods can be attributed to the LASO NPs incorporated in the polystyrene matrix. In comparison to the uncoated wood substrate, the coated LASO-PS nanocomposite film displayed also photostability and high durability. The current study proved potential high-scale manufacturing of smart wood for a number of applications, such as safety directional signs in buildings, household products, and smart windows.

This article has been accepted for publication and undergone full peer review but has not been through the copyediting, typesetting, pagination and proofreading process which may lead to differences between this version and the Version of Record. Please cite this article as doi: 10.1002/bio.4137

Keywords: Smart wood; Aluminum strontium oxide; Nanocomposite; Long-persistent luminescence; Superhydrophobicity.

1. Introduction

Stimuli-responsive products are materials that respond by switching their behaviors to an external stimulus, such as light, chemicals and solvent polarity [1–3]. Both of phosphorescence and fluorescence are two forms of light-induced emissive luminescence. If this light-induced emission disappears right after the ultraviolet excitation source is switched off; then the case is fluorescence. If the emission lingers; then the case is afterglow phosphorescence which may continue for fractions of a second or even few seconds (phosphorescence) up to few hours (long-persistent photoluminescence) [4]. Long-lasting photoluminescence has been an important light-responsive observable fact utilized in the fabrication of smart commodities with the ability to emit light in darkness after excitation with an external light source, such as an ultraviolet device [5], sunlight and even visible indoor light . Long-lasting luminescence was utilized for different purposes, such as safety signs that have been developed as paints or strips to lead public to a secure place in emergency cases such as fire and electricity blackout [5–7]. Long-lasting luminescence can be attributed to the high capacity of a material to store light upon irradiation with an excitation light source. Then, this material continues releasing the stored energy for an extended time periods [8]. Currently, different long-lasting phosphors of different colors have been developed as primary emitters, such as Y_2O_2S: Mg^{2+}, Ti^{4+} for red emission [9], $SrAl_2O_4$: Eu^{2+},Dy^{3+} for greenish emission [10], and $CaAl_2O_4$: Eu^{2+},Nd^{3+} for bluish emission [11]. Those long-lasting inorganic phosphors are characterized by high quantum yield, bright colors, high reversibility, and high thermal, chemical and photostability. Long-lasting rare earth doped phosphors are of particular interest [12–14]. They have been used in the fabrication of many commercial commodities, such as optical sensors, light emitting diodes, luminous indicators, emissive displays, switches and smart textiles [15–17]. Amongst them, the lanthanide-doped aluminum strontium oxide (LASO; $SrAl_2O_4$: Eu^{2+}, Dy^{3+}) has been an outstanding phosphor due to its distinguished characteristics, such as long-lasting phosphorescence (>10 hours), non-radioactivity, non-toxicity, high brightness and recyclability [18,19]. In general, long-lasting photoluminescent materials consist of two key constituents, including crystals of collective elements and light traps [20]. The crystal is the photoluminescent ingredient which can be charged upon excitation with light energy, while the traps have the long-lasting ability to hold the stored light for extended time periods. Thus, the

crystals continue discharging light after excitation. This extended time periods of light phosphorescence is supported by the traps, such as Eu^{2+} and Dy^{3+} [21].

Wood structure is distinguished by porous and fibrous tissue scaffolds observed in both stems and roots of wooden plants. It consists of cellulosic fibrous entities dispersed in lignin bulkiness. It has been utilized in many fields, such as paper industry, flooring, furniture, boats, shelters and houses [22,23]. Coated woods have been more interesting in the fabrication of smart commodities owing to its low thermal conductivity, high optical transmittance and mechanical toughness. Thin coatings are two dimensional functional films characterized by large surface area, high flexibility and light weight. These advantages result in improved elasticity, tensibility and strength in comparison to the corresponding three dimensional bulk substrates [24,25]. Thin coatings have been important for a range of applications, such as filters, electronic devices, drug delivery, antireflective coatings and photovoltaics. This can be attributed to their economical processing employing small quantities of raw materials [26,27]. Nano-scaled materials have been utilized to present innovative features to polymer substrates [28–35]; therefore, composite coatings immobilized with nano-scaled materials have particularly attracted high interest owing to their significant characteristics, such as transparency, water-repellency, electrical conductivity and optical and antimicrobial advantages [36,37]. Nano-scaled materials have been applied as fillers in different matrices as they have a great ability to maintain transparency of those matrices [36,37]. Thus, nanocomposite coatings have been appropriate substrates for a variety of advanced applications. Different surface coatings have been reported for woods to enhance their performance, such as avoiding environmental degradation and physical damages, in addition to enhancing their mechanical, thermal and functional properties [38]. However, luminescent woods with high photostability still require the development of innovative coatings with improved mechanical characteristics. Polymer nanocomposite coatings have demonstrated excellent mechanical characteristics in terms of hardness and toughness [39–43]. In order to build up efficient organic/inorganic nanocomposite coatings, inorganic nanoparticles such as graphite, nanoclay and carbon nanotubes have been applied as fillers in a polymer matrix for a variety of functional applications such as textiles, foodstuff packaging, cosmetics, pharmaceutics and optics [44]. Polystyrene is a commercial glassy thermoplastic polymer characterized by a variety of physical features, such as high dimensional stability, high-quality strength, as well as good electrical and thermal performance. Hence, polystyrene has been utilized for various fields, such as foodstuff packaging, automobile parts, appliances and electronics [45–48]. Polystyrene films are distinguished by good light-transmittance and high stability to aging even at high temperatures;

thus, they have been broadly used for many optical devices, such as optical data storage discs [49–51].

The production of long-lasting photoluminescence wood by coating with a nanocomposite of polystyrene and LASO NPs has not been reported yet. Herein, we study the first example of long-lasting photoluminescent and superhydrophobic coated wood for a diversity of potential applications, such as safety signs, gentle indoor and outdoor lighting, decorations and smart windows. The present study presents a simple strategy toward the development of glow-in-the-dark coated woods with high hardness, photostability, reversibility and low-cost. The long-lasting photoluminescence woods were prepared by coating with a nanocomposite of polystyrene and LASO NPs. The decay time and photoluminescence properties were explored. The LASO NPs were investigated by TEM, while the morphological features of coated woods were studied by SEM, EDX and XRF. The coated woods showed different colors underneath diverse circumstances. Those colors included colorless underneath the visible light, intense green underneath UV, and greenish in the dark. This was proved by CIE Lab coordinates, and UV-Vis absorption and emission spectral results. The superhydrophobic properties and surface toughness were also explored. The current coating can be applied to woods toward a variety of potential commercial applications, such as household products, safety directional signs in buildings, and smart window. The current concept can be utilized to provide different lightening conditions in buildings and household products, such as windows, curtain walls, pavements and parks, as well as directional signs on highways and streets. This will allow reducing energy consumption toward green and sustainable building environments.

2. Experimental section

2.1. Materials

Basswood slabs (2 mm thickness, 7.5 cm length and 2.5 cm wideness) were supplied from the local market in Egypt. The materials applied in the preparation of LASO, including boric acid, aluminum oxide, strontium carbonate, dysprosium oxide and europium oxide were obtained from Sinopharm Ltd, China. Polystyrene (280 kDa) and toluene (solvent to disperse polystyrene and LASO NPs) were obtained from Aldrich.

2.2. Preparation of LASO NPs

According to previous procedure [52], a mixture of strontium carbonate (100 mmol), dysprosium oxide (1 mol), boric acid (20 mmol), aluminum oxide (200 mmol) and europium oxide (2 mmol) was stirred in absolute ethanol (250 mL), and homogenized for about an hour by ultrasonic (25 kHz; Sonics Vibra-Cell Ultrasonicator) to guarantee a homogeneous dispersion.

After drying at 90°C over 24 hrs, the admixture was crushed by a planetary ball mill system for 3 hrs, and exposed to sintering at 1300°C over 3 hrs under a reductive carbon environment. The generated fine particles were milled and exposed to sieving to provide LASO micro-scaled particles (9-28 μm). To guarantee a better dispersion of LASO particles, it was further grinded by the top-down method to produce LASO NPs [53]. Thus, the micro-scaled LASO particles (10.0 g) were put into a ball mill (stainless steel; 20 cm) on a vibrating bar. An additional SiC ball mill (0.1 cm) was repeatedly smashed with the LASO micro-scaled powder in the stainless steel vial and the vibrating slab for 24 hrs to produce LASO NPs.

2.3. Preparation of luminescent coated wood

In order to develop LASO-PS nanocomposite coating, toluene (30 mL) was applied as a solvent to disperse the LASO NPs at different ratios, including zero, 0.05, 0.1, 0.5, 1, 2, 4, 6, 8, 10, 12 and 14 wt% (relative to the mass of polystyrene); represented by LASO-PS-0, LASO-PS-1, LASO-PS-2, LASO-PS-3, LASO-PS-4, LASO-PS-5, LASO-PS-6, LASO-PS-7, LASO-PS-8, LASO-PS-9, LASO-PS-10 and LASO-PS-11, respectively. Each admixture was stirred for about an hour and homogenized (35 kHz) for 15 minutes. PS (3 g) was then added to each admixture, stirred for about an hour, and homogenized (25 kHz) for 15 minutes to guarantee a complete dissolution of PS in toluene and homogeneous dispersion of LASO NPs in the PS solution to afford the corresponding LASO-PS nanocomposites. The wood substrates were immersed in the produced LASO-PS nanocomposite for 1-2 minutes, and dried at 120 °C over 2 hrs. The immersion/drying procedures were repeated three times to give the corresponding long-lasting luminescent wood sample.

2.4. Characterization analysis

2.4.1. Morphologies measurements

The SEM images were taken by Quanta (Czech) coupled to EDX TEAM analyzer to determine the elements contents of the coated woods. The chemical compositions of the coated woods were also determined by Axios Sequential XRF. The particle size and morphology of LASO NPs were studied by JEOL 1230 TEM (Japan). The LASO NPs were firstly dispersed in distilled water and homogenized (25 kHz) over 15 minutes for TEM analysis.

2.4.2. Hydrophobic properties

The water contact angle was studied by OCA15EC Dataphysics (Germany) employing 10 μL of water drops.

2.4.3. Mechanical measurements

The resistance to scratching and tensile strength of the composite films were investigated using HB scratch pencils and Shimadzu universal tensile testing instrument (ASTM D638M), respectively.

2.4.4. Photoluminescence properties

The UV-Vis absorbance and emission spectral curves were investigated by FP-8300 JASCO coupled with phosphorescence accessory to study the decay time. The photoluminescent wood substrates were irradiated at 365 nm utilizing an UV deice (6 W).

2.4.5. Reversibility

The photostability of the coated wood was studied by irradiation with UV at 365 nm for 5 minutes. The coated wood was left in a dark box for 100 minutes to discharge light. The emission intensity was measured before and beneath the irradiation with UV over several cycles.

2.4.6. Colorimetric studies

CIE Lab and color intense (*K/S*) of the blank and treated woods were studied by Ultra-Scan-Pro Hunter Lab (United States). The wood substrate was irradiated to UV, and then the colorimetric properties were determined before and beneath the irradiation with UV. Photos of LASO-PS-9 wood were reported by Canon (A710IS) camera.

3. Results and discussion

3.1. Fabrication of long-lasting luminescent wood

Different ratios of LASO NPs were dispersed in toluene, stirred and homogenized by ultrasonic to achieve a homogeneous dispersion. PS was added to each suspension, and the admixture was stirred, and then homogenized to give the corresponding LASO-PS composite. Wood substrates were dip-coated in the produced LASO-PS composites. To facilitate the preparation of luminescent translucent coating, the prepared LASO micro-scaled particles were initially subjected to the top-down grinding to provide the nano-scaled particles [21]. The particle

diameter was evaluated by TEM images to illustrate a diameter of 14-23 nm as depicted in **Figure 1**.

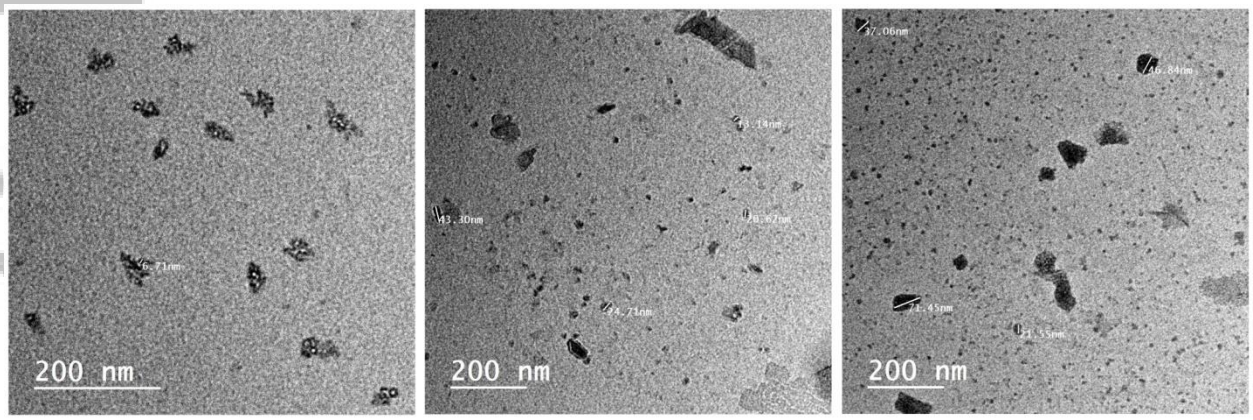

Figure 1. TEM photos of LASO nano-scaled particles.

3.2. Morphological measurements

SEM images (**Figure 2**) showed that no substantial differences were detected between LASO-PS-0 and the luminescent woods demonstrating a smooth surface with lowest roughness which was found to increase with increasing the ratio of LASO NPs. However, the uncoated wood demonstrated a fibrous surface **(Figure 2)**. Furthermore, no differences were detected on the coated surfaces with increasing LASO NPs. The existence of the rare earth doped aluminum strontium oxide within the coated polystyrene layer was verified by studying the elemental compositions of the coated film using EDX spectral analysis as demonstrated in **Figure 3**. **Table 1** illustrates the chemical contents of LASO-PS-9 at three selected sites on the wood surface to show similar ratios of elements verifying a homogeneous dispersion of LASO NPs within the surface coating. The elemental mapping of LASO-PS-9 was also explored to show a consistent dispersion of LASO NPs on the coated film. The elemental ratios of the monitored elements matched their ratios used in the preparation of the composite integrated with LASO. The luminescent coating consisted of polystyrene (C and O) as the major hosting bulk and LASO (Sr, Al, Dy and Eu) as the minor trapped material.

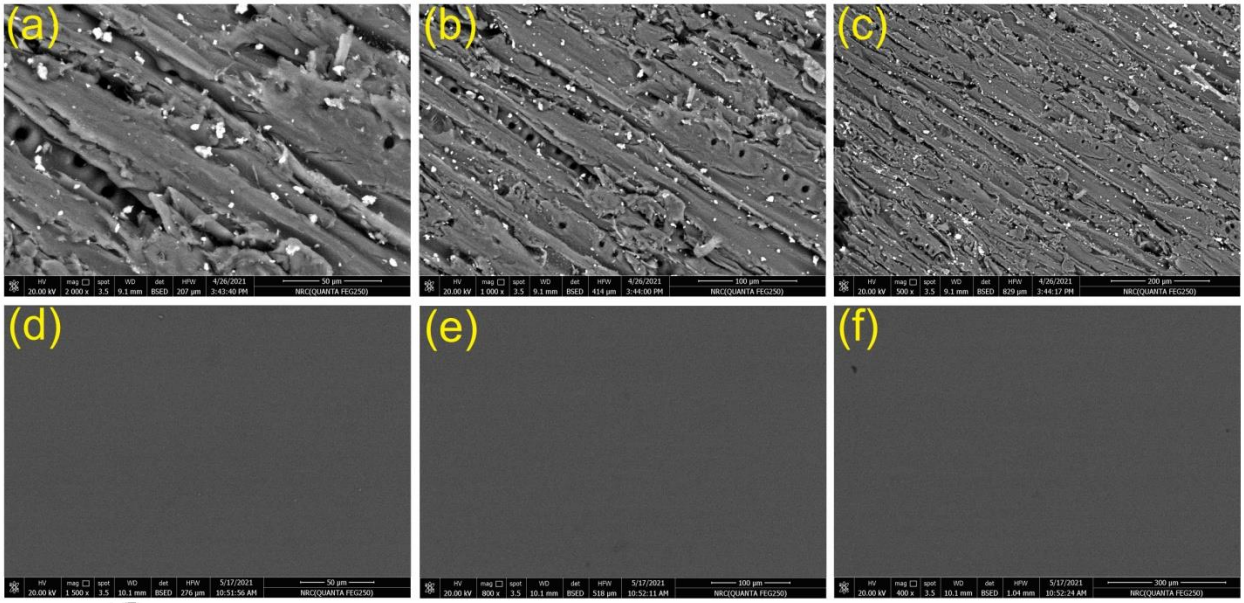

Figure 2. SEM images of LASO-PS-0 (a, b, c), and LASO-PS-9 (d, e, f).

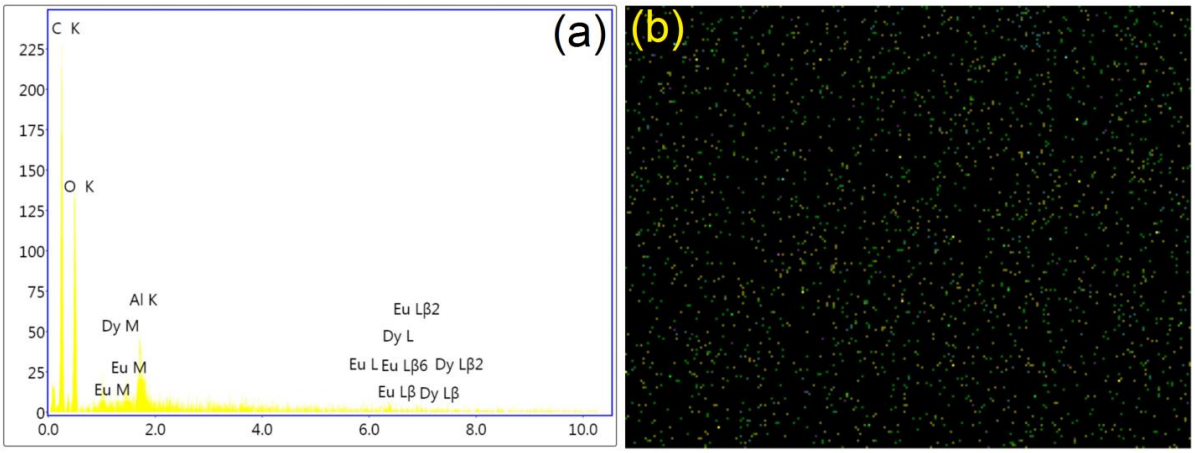

Figure 3. EDX spectra (a) and mapping (b) of LASO-PS-9.

Table 1. Chemical compositions (wt%) of LASO-PS-0, LASO-PS-1, LASO-PS-9 and LASO-PS-11 at three selected sites (S_1, S_2 and S_3) on the sample surface.

Wood		C	O	Al	Sr	Eu	Dy
LASO-PS-0	S_1	58.54	41.46	0	0	0	0
	S_2	58.65	41.35	0	0	0	0

	S_3	58.89	41.11	0	0	0	0
LASO-PS-1	S_1	57.13	40.33	1.12	0.86	0.20	0.16
	S_2	57.15	40.17	1.15	0.94	0.25	0.14
	S_3	57.22	40.10	1.19	0.84	0.24	0.11
LASO-PS-9	S_1	55.28	38.63	2.82	1.83	0.83	0.61
	S_2	55.12	39.01	2.71	1.72	0.85	0.59
	S_3	55.34	38.60	2.80	1.79	0.78	0.68
LASO-PS-11	S_1	54.23	37.16	3.41	2.82	1.35	1.03
	S_2	54.17	37.19	3.44	2.88	1.28	1.04
	S_3	54.11	37.25	3.47	2.83	1.33	1.01

Both XRF and EDX have been applied to determine the elemental compositions of a definite surface. Nonetheless, XRF typically reports the elemental compositions with an identification limit >10 mg/kg. EDX is a superior system that has been used to determine the elemental compositions of a definite surface at a higher detection limit and lower error [54]. XRF spectra of LASO-PS-9 (surface area of 1.88 cm^2) detected only SrO (35.42 w%) and Al_2O_3 (64.58 w%). However, the remarkably low contents of Eu and Dy were not detected by XRF. The elemental constitution of LASO was studied by XRF and EDX, which matched with their corresponding ratios used in the composite preparation.

3.3. Mechanical behavior

The mechanical performance is a major feature that influences the durability of the coated wooden substrates. The key inspiration of selecting polystyrene as a coating matrix was to accomplish a smooth photoluminescent surface at high transparent appearance and lowest roughness [55,56] Thus, both of scratching and tensile tests were investigated to inspect the mechanical performance of the coated luminescent films. Both blank and coated woods were exposed to the scratching test to inspect their scratching resistance. The scratching pencil hardness examination method has been an effective practice to assess the scratching resistance of films [57]. Scratching pencils with hardness in the range of 6B-9H were initially sharpened and utilized to scratch the composite film coated on the wood samples. The uncoated wood substrate could not uphold their resistance to scratching beyond the 6B pencil hardness. LASO-PS-0 was capable to resist scratching up to 3B pencil. However, the wood substrates, from LASO-PS-1 to LASO-PS-11, were capable to resist scratching up to B, HB, HB, F, F, H, 2H,

3H, 4H, 4H and 4H, respectively. Therefore, an improved resistance to scratching was observed upon increasing the ratio of LASO NPs. The effect of the LASO ratio on the tensile strength (TS) of the PS film is demonstrated in **Figure 4**. LASO improved the TS of the PS film owing to the high surface area of LASO NPs, which acted as a stress transferring mediator in the composite. This induced plastic deformation in the PS film; and therefore, enhanced the TS. Therefore, the TS of the PS film increased upon increasing LASO ratio. The enhanced TS of the PS films can also be ascribed to the development of intermolecular hydrogen bonding among the wood cellulose and polystyrene. This facilitates the creation of 3D polystyrene network entrapping the LASO nanoparticles on the wood surface [58,59]. Thus, the development of 3D network could be enhanced by aluminum existing in the elemental composition of LASO, which can function as a coordination cross-linker among the negative charges on PS surface leading to a higher molecular weight 3D network [60,61].

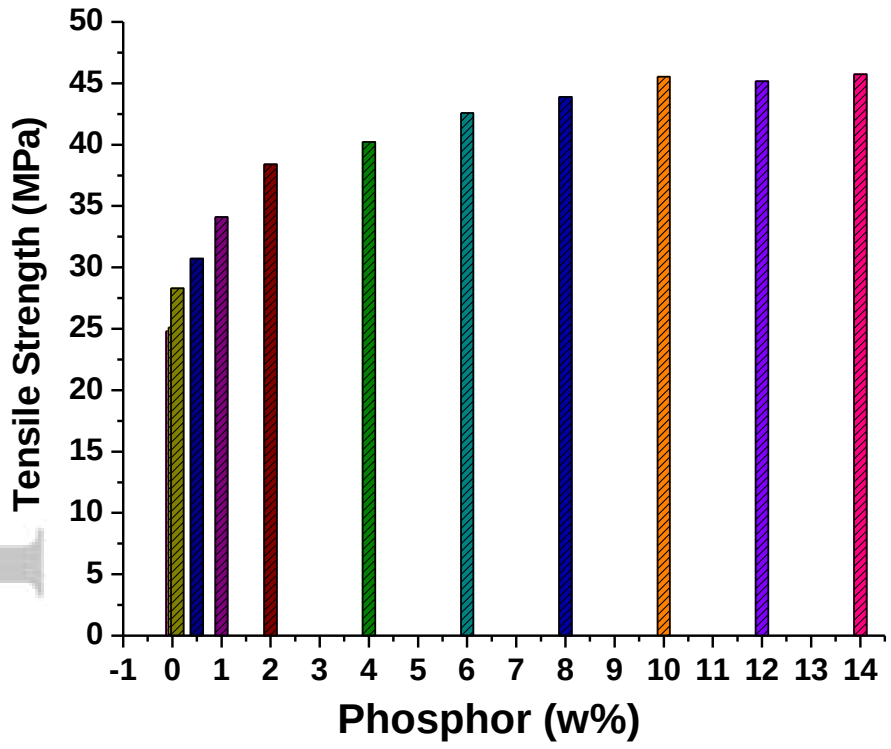

Figure 4. TS of LASO-PS composite films.

3.4. Hydrophobic properties

The contact angle was determined and summarized in **Table 2**. We were not able to determine a water contact angle for the uncoated wood. LASO-PS-0 displayed an average contact angle of 98.4°, which improved to 118.6° for LASO-PS-1 owing to the inclusion of LASO NPs. The

values of contact angles increased from 118.6° to 152.6° with raising the ratio of LASO from LASO-PS-1 to LASO-PS-8, which can be attributed to the improved film roughness. Nonetheless, the contact angles were almost stable with raising the ratio of LASO from LASO-PS-8 to LASO-PS-11. This can be attributed to the highly increased ratio of LASO NPs to result in decreasing the surface roughness due to the highly decreased spaces between LASO NPs.

Table 2. Hydrophobic screening of the wooden samples.

Wood	Contact angle (°)
LASO-PS-0	98.4
LASO-PS-1	118.6
LASO-PS-2	125.2
LASO-PS-3	134.2
LASO-PS-4	139.3
LASO-PS-5	144.5
LASO-PS-6	148.7
LASO-PS-7	151.1
LASO-PS-8	152.6
LASO-PS-9	152.5
LASO-PS-10	152.6
LASO-PS-11	152.4

3.5. Coloration measurements

To generate a translucent film on a wood substrate, LASO NPs must be dispersed efficiently in PS. The luminescent woods with lowest ratio of LASO, from LASO-PS-1 to LASO-PS-3, were capable to produce bright green color only under UV irradiation. This color was instantly disappeared upon removing the UV source to indicate ultraviolet-induced fluorescence-based photochromism. On the other side, the woods with higher ratios of LASO, from LASO-PS-4 to LASO-PS-11, displayed green emission beneath UV source and continued to emit light in the dark indicating long-lasting phosphorescence. The luminescent films demonstrated a transparent appearance as the coated woods showed a brown color similar to the uncoated

wood. Small differences were detected in *K/S* **(Table 3)** beneath the daylight with raising LASO, from LASO-PS-0 to LASO-PS-11, verifying the transparency of the composite coating film. Similarly, slight increase was detected in *K/S* under UV compared to that beneath the visible daylight to designate a color shift of the transparent LASO-PS to bright green. *K/S* increased with increasing the ratio of LASO to indicate the generation of greener shades **(Figure 5)**.

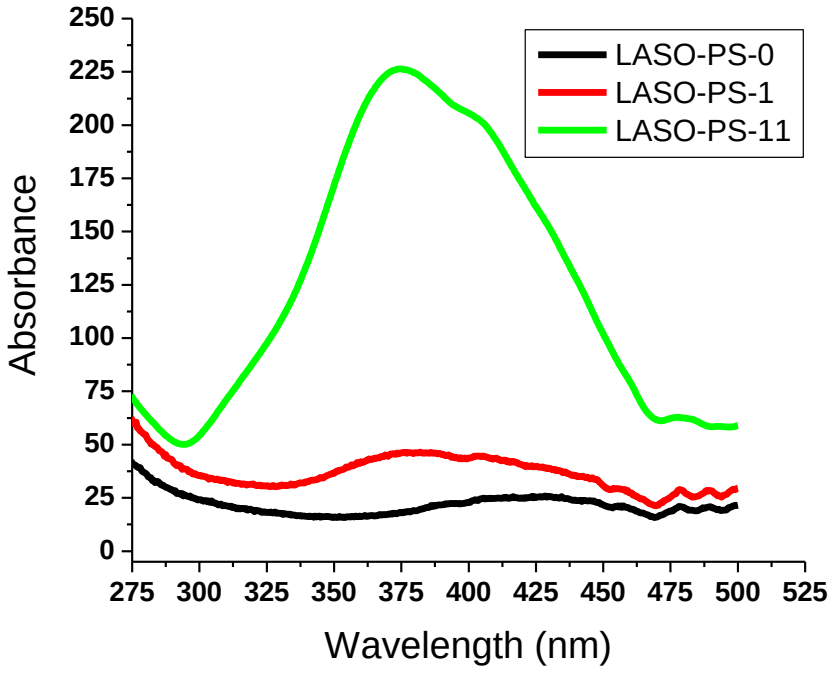

Figure 5. Absorption spectral curves of LASO-PS coated woods.

The absorbance maxima of LASO-PS were detected at 374 nm owing to the colorless character of the composite films, while the emission maxima were detected at 518 nm to designate a bright green color. LASO-PS-0 displayed slight differences in L*, a* and b*. Underneath the visible daylight, the luminescent woods demonstrated considerable differences in L*, a* and b* with increasing the ratio of LASO. L* decreased at the higher ratios of LASO due to the color change from colorless (LASO-PS-1 to LASO-PS-9) to slightly off-white (LASO-PS-10 to LASO-PS-11). Underneath UV, L* decreased as a result of increasing the green shade monitored at the higher ratios of LASO. Underneath the visible daylight, negligible differences were observed in -a* and +b* at the higher ratios of LASO to confirm transparency of the composite film. Underneath the UV source, both -a* and +b* increased compared to the corresponding values underneath the visible daylight due to the color change from colorless to

green. With increasing the ratio of LASO, the -a* increases and +b* decreases underneath UV source due to the LASO ratio-dependent greener color. Instantaneously after removing away the UV device, the luminescent woods, from LASO-PS-1 and LASO-PS-3, instantly retrieved their brown status to signify fluorescence emission. On the other side, the luminescent woods, from LASO-PS-4 and LASO-PS-11, showed long-lasting phosphorescence emission together with the increased -a* and +b* values. Nonetheless, small increments were detected with increasing LASO more than LASO-PS-9 to indicate that the best long-lasting emission was monitored for LASO-PS-9.

Table 3. Coloration screening of wooden samples under visible (Vis) and (UV) lights.

Parameters		**0%**	**0.05%**	**0.1%**	**0.5%**	**1%**	**2%**	**4%**	**6%**	**8%**	**10%**	**12%**	**14%**
K/S	Vis	0.56	0.73	0.79	0.82	0.91	0.97	1.01	1.07	1.13	1.25	1.40	1.56
	UV	0.49	1.42	1.50	1.62	1.73	1.86	2.05	2.33	2.50	2.63	2.75	2.98
L^*	Vis	79.55	78.50	78.12	77.71	76.53	74.23	72.44	69.18	65.05	65.00	64.04	63.86
	UV	78.03	69.81	68.73	65.50	65.67	63.90	62.14	59.82	57.73	57.42	57.07	56.84
a^*	Vis	-1.02	-0.91	-0.84	-0.76	-0.73	-0.69	-0.64	-0.50	-0.40	-0.36	-0.28	-0.17
	UV	-1.00	-2.93	-3.08	-3.22	-3.52	-3.85	-3.96	-4.8	-5.26	-6.21	-7.52	-8.05
b^*	Vis	1.34	1.88	1.98	2.12	2.42	2.88	3.02	3.44	3.90	4.00	4.25	4.47
	UV	1.39	10.85	10.28	9.83	9.75	8.70	7.53	6.71	6.24	5.91	5.73	5.30

3.7. Photoluminescence spectra

The brown background of the coated wood substrates was found to enhance the optical identification of the color change to intense green under the ultraviolet device, and green-yellow in the dark **(Figure 6)**. The luminescent woods, from LASO-PS-1 to LASO-PS-3, showed fluorescence emission beneath ultraviolet lamp with immediate reversibility upon removing the lamp. Thus, those fluorescent woods displayed no emission directly after removing away the UV lamp. The luminescent woods, from LASO-PS-4 to LASO-PS-11, with higher ratios of LASO demonstrated slow reversibility and glow-in-the-dark indicating long-lasting luminescence. After excitation with ultraviolet, the decreased absorption and emission intensities of LASO-PS-9 were followed versus time **(Figure 7)**. The absorption intensity was detected to increase at 374 nm with increasing the irradiation time (5-80 seconds). On the other side, two emissions were detected at 434 and 518 nm. The intensity at 434 nm was stable versus time, while the intensity at 518 nm proportionally increased versus time. This was associated with a color change from brown to green under UV, and to greenish-yellow in the dark. PS

acted as an organic matrix trapping LASO NPs. No major effects were observed in the photoluminescence performance of the coated woods which demonstrated optical activity almost identical to that of LASO NPs [62].

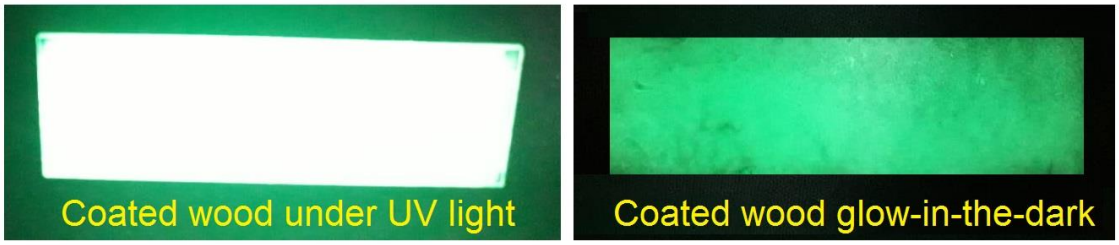

Figure 6. Images of LASO-PS-9 under UV light (*left*), and glow-in-the-dark (*right*); the sample dimensions were 2 mm thickness, 7.5 cm length and 2.5 cm wideness.

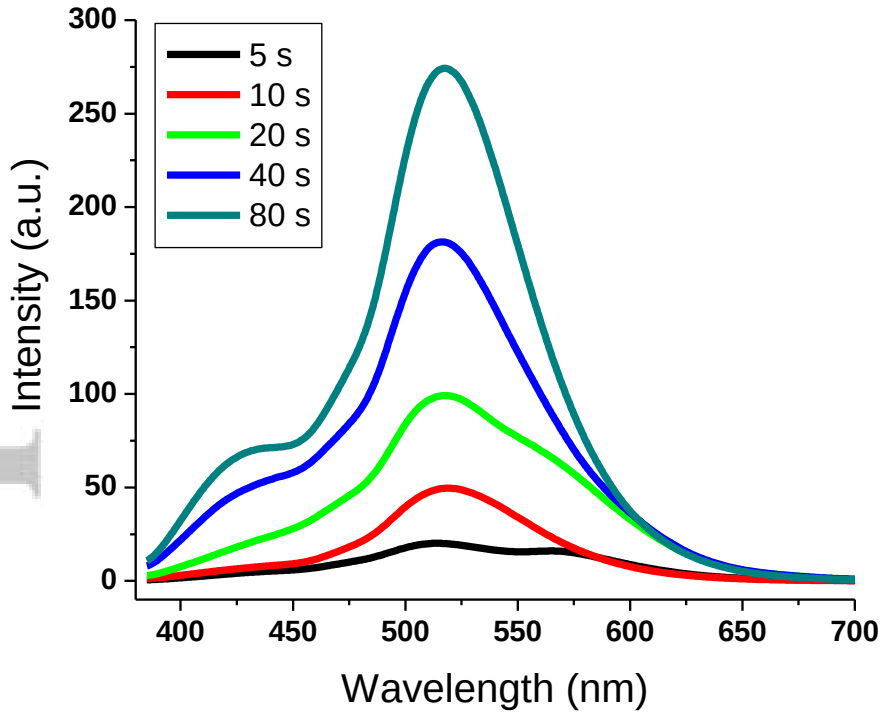

Figure 7. Emission spectral curves of LASO-PS-9 after excitation with UV for several time periods (5-80 s).

The LASO emission typically arises from $4f^6 5D^1 \leftrightarrow 4f^7$ transition of Eu^{2+} ions. No emission band was detected for Eu^{3+} to prove a complete switch to Eu^{2+}. This also proved that energy absorbed by Dy^{3+} transfered to Eu^{2+}. Dy^{3+} has the ability to motivate the creation of traps to be transported into Eu^{2+}, and then discharged or glow upon reverting Eu^{2+} to its ground state [63–65] Durable luminescent materials typically have excellent reversibility to fatigue upon applying coloration/discoloration process, which can be explored by studying the emission variations occurring to LASO-PS-9 at 518 nm. LASO-PS-9 was evaluated over repeated cycles of excitation to UV for 5 minutes and darkness for 100 minutes. The emission intensity was measured at 518 nm under UV and after 100 minutes in darkness. High photostability was observed without deterioration as shown in **Figure 8**.

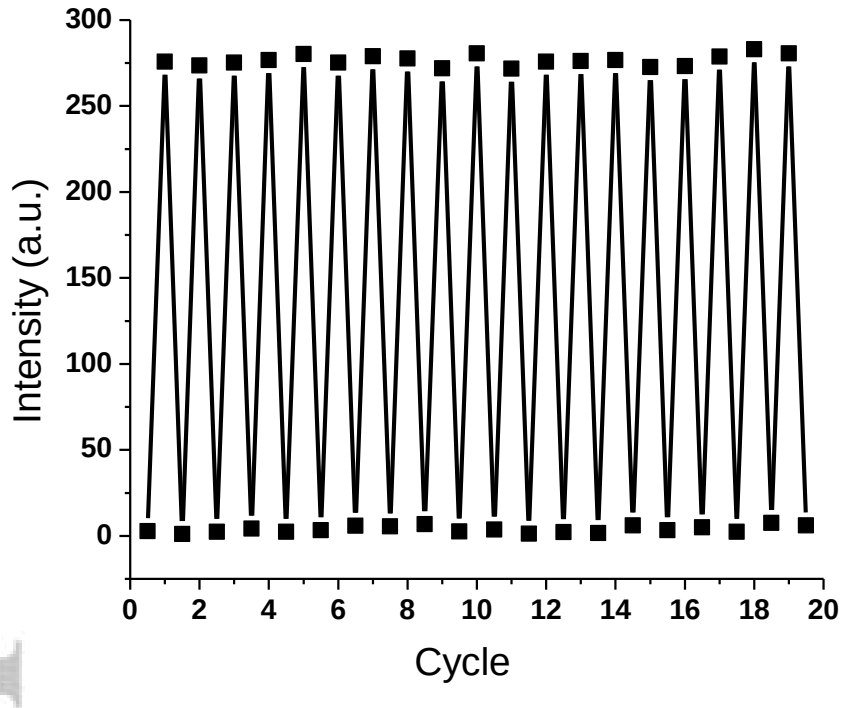

Figure 8. Emission intensities of LASO-PS-9 at 518 nm under UV and after 100 minutes in darkness.

The emission maxima were monitored at 508 nm, which is slightly less than that of LASO NPs [54]. The absorption curve was detected in the range of 290-475 nm, while the emission curve was in the area of 375-650 nm. The decay time exhibited a non-linear relationship versus time as shown in **Figure 9**. The long-lasting emissive decay exhibited two stages. The primary stage was faster owing to the short time needed to keep electrons in the excitation status of Eu^{2+}, while the second stage was slow owing to the shallow and deeply trapped energy centers of

Dy^{3+}. Lanthanides have been monitored as ionic trapping entities with high capacity to increase the exhausting time of light. Hence, the intensity of phosphorescence associated basically to the amount of ionic traps; whilst the persistent time depends on how deeply is the trapped energy [66,67].

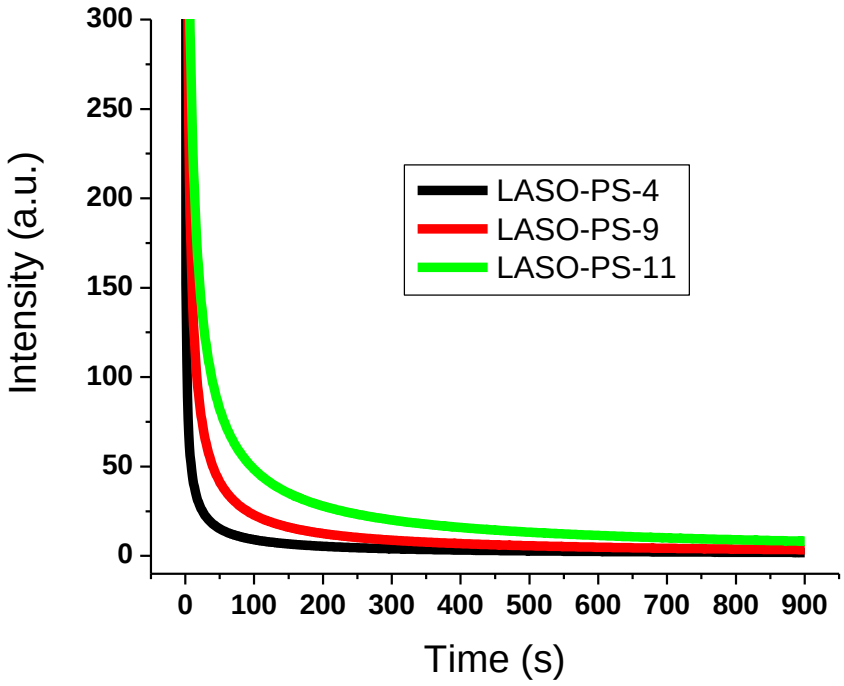

Figure 9. Decay time of some selected coated woods.

4. Conclusions

In summary, we successfully developed long-lasting photoluminescent and hydrophobic woods coated with a polystyrene composite immobilized with nanoparticles of lanthanide-doped aluminum strontium oxide. The coated woods displayed fluorescence photochromism at the lower ratios of the luminophore as high as 0.5 wt%. Long-lasting phosphorescence was detected at the higher ratios of the lanthanide-doped luminophore as low as 0.75 wt%. The phosphor nano-scaled particles were evaluated by TEM to show diameters of 14-23 nm. The morphologies were studied by XRF, EDX and SEM. The hydrophobic activity was also explored by recording the changes in the water contact angle with increasing the ratio of the phosphor nanoparticles to demonstrate an increased hydrophobic activity of 98.4-152.6°. As confirmed by decay time, CIE Lab measurements and emission/excitation spectral curves, the composite coating exhibited a color shift from colorless (374 nm) to green (518 nm) under UV and to green-yellow in the dark. The coated woods demonstrated high reversibility, durability

and photostability. The mechanical performance, including resistance to scratching and tensile strength, of the composite coatings were screened to display improvements with increasing the phosphor ratio. The current study showed a good approach to develop multifunctional coatings onto wood substrates, which can be easily applied to other surfaces such as metals and ceramics, toward a potential industrial manufacturing for a diversity of applications, such as emergency signs and energy-saving smart windows.

Acknowledgements

The authors acknowledge King Saud University, Riyadh, Saudi Arabia, for funding this work through Researchers Supporting Project number (RSP-2021/30).

Competing Interests

The author declares that there is no conflict of interest regarding the publication of this paper.

References

[1] Y. Du, D. Yang, S. Sun, Z. Zhao, D. Tang, *Luminescence*. **2015** ,30 519–525.

[2] S.K. Mellerup, S. Wang, *Chem. Soc. Rev.* **2019** ,48 3537–3549.

[3] T.A. Khattab, *Mater. Chem. Phys.* **2020** 123456.

[4] T.A. Khattab, B.D.B. Tiu, S. Adas, S.D. Bunge, R.C. Advincula, *Dye. Pigment.* **2016** ,130 327–336.

[5] Q. He, G. Qiu, X. Xu, J. Qiu, X. Yu, *Luminescence*. **2015** ,30 235–239.

[6] Y. Li, M. Gecevicius, J. Qiu, *Chem. Soc. Rev.* **2016** ,45 2090–2136.

[7] R. Kabe, C. Adachi, *Nature*. **2017** ,550 384–387.

[8] Z. Wang, Y. Zhang, C. Wang, X. Zheng, Y. Zheng, L. Gao, C. Yang, Y. Li, L. Qu, Y. Zhao, *Adv. Mater.* **2020** ,32 1907355.

[9] W. Li, Y. Liu, P. Ai, *Mater. Chem. Phys.* **2010** ,119 52–56.

[10] W. Shan, L. Wu, N. Tao, Y. Chen, D. Guo, *Ceram. Int.* **2015** ,41 15034–15040.

[11] T. Cui, P. Ma, Y. Sheng, K. Zheng, X. Zhou, C. Xu, H. Zou, Y. Song, *Opt. Mater. (Amst).* **2017** ,67 84–90.

[12] J. Wang, Q. Ma, Y. Wang, H. Shen, Q. Yuan, *Nanoscale*. **2017** ,9 6204–6218.

[13] Y. Mu, M. Qiu, X. Zhou, Q. Li, M. Sun, H. Yang, W. Fu, L. Yang, J. Ma, *Luminescence*. **2015** ,30 503–506.

[14] A.N. Yerpude, S.J. Dhoble, *Luminescence*. **2012** ,27 450–454.

[15] X. Sun, L. Song, N. Liu, J. Shi, Y. Zhang, *ACS Appl. Nano Mater.* **2021**.

[16] L. Liang, N. Chen, Y. Jia, Q. Ma, J. Wang, Q. Yuan, W. Tan, *Nano Res.* **2019** ,12 1279–1292.

[17] V. Vitola, D. Millers, I. Bite, K. Smits, A. Spustaka, *Mater. Sci. Technol.* **2019** ,35 1661–1677.

[18] V. Havasi, D. Tátrai, G. Szabó, E. Varga, A. Erdőhelyi, G. Sipos, Z. Kónya, Á. Kukovecz, *J. Lumin.* **2020** ,219 116917.

[19] G.I. Akmehmet, S. Šturm, M. Komelj, Z. Samardžija, B. Ambrožič, M. Sezen, M. Čeh, C.W. Ow-Yang, *Ceram. Int.* **2019** ,45 20073–20077.

[20] T.A. Khattab, M. Rehan, Y. Hamdy, T.I. Shaheen, *Ind. Eng. Chem. Res.* **2018** ,57 11483–11492.

[21] M.M. Abdelhameed, Y.A. Attia, M.S. Abdelrahman, T.A. Khattab, *Luminescence*. **2021** ,36 865–874.

[22] Z. Li, T. Zhan, M. Eder, J. Jiang, J. Lyu, J. Cao, *J. Wood Sci.* **2021** ,67 1–6.

[23] S. Tian, H. He, P. Yu, L. Zhou, Y. Luo, D. Jia, *J. Clean. Prod.* **2017** ,164 840–847.

[24] M.M. Ghafurian, H. Niazmand, E.K. Goharshadi, B.B. Zahmatkesh, A.E. Moallemi, R. Mehrkhah, O. Mahian, *Desalination*. **2020** ,493 114657.

[25] A. Cogulet, P. Blanchet, V. Landry, P. Morris, *Int. Biodeterior. Biodegradation*. **2018** ,129 33–41.

[26] D.L. Zhao, S. Japip, Y. Zhang, M. Weber, C. Maletzko, T.-S. Chung, *Water Res.* **2020** ,173 115557.

[27] G.S. Lai, W.J. Lau, P.S. Goh, A.F. Ismail, Y.H. Tan, C.Y. Chong, R. Krause-Rehberg, S. Awad, *Chem. Eng. J.* **2018** ,344 524–534.

[28] J. Hussein, M. El-Bana, E. Refaat, M.E. El-Naggar, *J. Funct. Foods*. **2017** ,37.

[29] M.H. El-Newehy, M.E. El-Naggar, S. Alotaiby, H. El-Hamshary, M. Moydeen, S. Al-Deyab, *J. Nanosci. Nanotechnol.* **2018** ,18 805–814.

[30] S. Sharaf, M.E. El-Naggar, *Cellulose*. **2018**.

[31] A. Hebeish, M.E. El-Naggar, S. Tawfik, S. Zaghloul, S. Sharaf, *Cellulose*. **2019** ,26 3543–3555.

[32] E.K. Radwan, H. Kafafy, S.T. El-Wakeel, T.I. Shaheen, T.A. Gad-Allah, A.S. El-Kalliny, M.E. El-Naggar, *Cellulose*. **2018** ,25 6645–6660.

[33] H.F. Youssef, M.E. El-Naggar, F.K. Fouda, A.M. Youssef, *Food Packag. Shelf Life*. **2019** ,22.

[34] M.E. El-Naggar, A.M. Abdelgawad, A. Tripathi, O.J. Rojas, *J. Environ. Chem. Eng.* **2017** ,5 5754–5761.

[35] M.K. Ahmed, M.E. El-Naggar, A. Aldalbahi, M.H. El-Newehy, A.A. Menazea, *J. Mol. Liq.* **2020** 113794.

[36] S. Giraldo, Z. Jehl, M. Placidi, V. Izquierdo-Roca, A. Pérez-Rodríguez, E. Saucedo, *Adv. Mater.* **2019** ,31 1806692.

[37] T.A. Khattab, M.E. El-Naggar, M.S. Abdelrahman, A. Aldalbahi, M.R. Hatshan, *Luminescence*. **2021** ,36 543–555.

[38] Z. Liao, X. Fang, J. Xie, Q. Li, D. Wang, X. Sun, L. Wang, J. Li, *ACS Appl. Mater. Interfaces.* **2019** ,11 5344–5352.

[39] D.L. Zhao, W.S. Yeung, Q. Zhao, T.-S. Chung, *J. Memb. Sci.* **2020** ,604 118039.

[40] M.E. El-Naggar, E.K. Radwan, S.T. El-Wakeel, H. Kafafy, T.A. Gad-Allah, A.S. El-Kalliny, T.I. Shaheen, *Int. J. Biol. Macromol.* **2018** ,113.

[41] A.M. Youssef, M.E. El-Naggar, F.M. Malhat, H.M. El Sharkawi, *J. Clean. Prod.* **2019** ,206.

[42] M.M.G. Fouda, N.R. Abdelsalam, I.M.A. Gohar, A.E.M. Hanfy, S.I. Othman, A.F. Zaitoun, A.A. Allam, O.M. Morsy, M. El-Naggar, *Colloids Surfaces B Biointerfaces.* **2020** ,188 110805.

[43] M.E. El-Naggar, M. Hasanin, A.M. Youssef, A. Aldalbahi, M.H. El-Newehy, R.M. Abdelhameed, *Int. J. Biol. Macromol.* **2020** ,165.

[44] C. Van Goethem, R. Verbeke, M. Pfanmöller, T. Koschine, M. Dickmann, T. Timpel-Lindner, W. Egger, S. Bals, I.F.J. Vankelecom, *J. Memb. Sci.* **2018** ,563 938–948.

[45] R. Abhijith, A. Ashok, C.R. Rejeesh, *Mater. Today Proc.* **2018** ,5 2139–2145.

[46] N.H. Ramli Sulong, S.A.S. Mustapa, M.K. Abdul Rashid, *J. Appl. Polym. Sci.* **2019** ,136 47529.

[47] Z. Liu, Y. Li, E. Pérez, Q. Jiang, Q. Chen, Y. Jiao, Y. Huang, Y. Yang, Y. Zhao, *J. Hazard. Mater.* **2021** ,402 123778.

[48] N.M. Ainali, D.N. Bikiaris, D.A. Lambropoulou, *J. Anal. Appl. Pyrolysis*. **2021** 105207.

[49] S. Thakur, A. Verma, B. Sharma, J. Chaudhary, S. Tamulevicius, V.K. Thakur, *Curr. Opin. Green Sustain. Chem.* **2018** ,13 32–38.

[50] B.T. Ho, T.K. Roberts, S. Lucas, *Crit. Rev. Biotechnol.* **2018** ,38 308–320.

[51] S. Cai, B. Zhang, L. Cremaschi, *Build. Environ.* **2017** ,123 50–65.

[52] K. Pavani, J.S. Kumar, K. Srikanth, M.J. Soares, E. Pereira, A.J. Neves, M.P.F. Graça, *Sci. Rep.* **2017** ,7 1–15.

[53] J. Fichtner, S. Watzele, B. Garlyyev, R.M. Kluge, F. Haimerl, H.A. El-Sayed, W.-J. Li,

F.M. Maillard, L. Dubau, R. Chattot, *ACS Catal.* **2020** ,10 3131–3142.
[54] T.A. Khattab, H. Abou-Yousef, S. Kamel, *Carbohydr. Polym.* **2018** ,200 154–161.
[55] T. Ghosh, N. Karak, *New J. Chem.* **2020** ,44 5980–5994.
[56] R. Yang, S. Zuo, B. Song, H. Mao, Z. Huang, Y. Wu, L. Cai, S. Ge, H. Lian, C. Xia, *Polymers (Basel).* **2020** ,12 2856.
[57] T. Sander, S. Tremmel, S. Wartzack, *Surf. Coatings Technol.* **2011** ,206 1873–1878.
[58] S. Dahle, J. Meuthen, R. Gustus, A. Prowald, W. Viöl, W. Maus-Friedrichs, *Coatings*. **2021** ,11 114.
[59] A. Can, H. Sivrikaya, B. Hazer, *Int. Biodeterior. Biodegradation*. **2018** ,133 210–215.
[60] H.M. Abumelha, *Luminescence*. **2021** ,36 1024–1031.
[61] S. Al-Qahtani, E. Aljuhani, R. Felaly, K. Alkhamis, J. Alkabli, A. Munshi, N. El-Metwaly, *Ind. Eng. Chem. Res.* **2021**.
[62] A.M. Atta, *Luminescence*. **2021** ,36 1078–1088.
[63] A. Aldalbahi, M.E. El-Naggar, T.A. Khattab, M. Hossain, *Luminescence*. **2021**.
[64] T.A. Khattab, M.M.G. Fouda, M.S. Abdelrahman, S.I. Othman, M. Bin-Jumah, M.A. Alqaraawi, H. Al Fassam, A.A. Allam, *J. Fluoresc*. **2019** ,29 703–710.
[65] O.M. Mokhtar, Y.A. Attia, A.R. Wassel, T.A. Khattab, *Luminescence*. **2021**.
[66] T.A. Khattab, M. Abd El-Aziz, M.S. Abdelrahman, M. El-Zawahry, S. Kamel, *Luminescence*. **2020** ,35 478–485.
[67] H.K. Alzahrani, A.M. Munshi, A.M. Aldawsari, A.A. Keshk, B.H. Asghar, H.E. Osman, M.E. Khalifa, N.M. El-Metwaly, *Luminescence*. **2021** ,36 964–976.

Facile production of smart superhydrophobic nanocomposite for wood coating toward long-lasting glow-in-the-dark photoluminescence

Mehrez E. El-Naggar[a*], Ali Aldalbahi[b], Tawfik A Khattab[a], Mokarram Hossain[c]

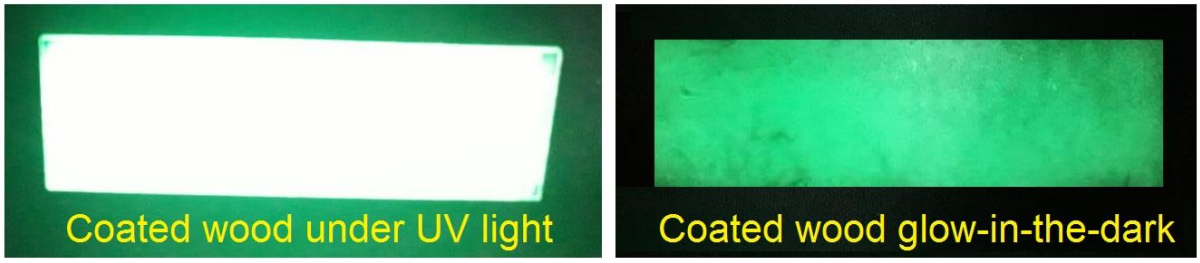

Photoluminescent coated wood was prepared for potential glow-in-the-dark superhydrophobic products. *Rare earth strontium aluminate dispersed in* polystyrene film was coated onto wood. Color changes were detected from brown under daylight to green under UV light. High photostability was monitored against UV light.